16. FACIES PATTERNS AND AUTHIGENIC MINERALS OF UPWELLING DEPOSITS OFF SOUTHWEST AFRICA[1]

G. Wefer,[2] W.H. Berger,[3] C. Richter,[4] and Shipboard Scientific Party[5]

ABSTRACT

Four different major sedimentary facies regimes were encountered during Ocean Drilling Program Leg 175. At the northern end of the north–south transect, off the mouth of the Congo River, sediments have a large terrigenous component. This is also true for sediments drilled off Angola, in sites close to the shelf edge, where very high sedimentation rates prevail. On and near Walvis Ridge, sediments have a strong pelagic aspect, although organic matter contents remain high. South of the ridge, in Walvis Bay and near Lüderitz Bay, sediments are unusually rich in opal and organic matter, reflecting the high coastal ocean productivity. At the southern end of the transect, in the Southern Cape Basin, sediments are dominated by pelagic carbonate deposition. Generally, organic carbon contents were quite high at all sites, ranging from a few percent to as much as 20%. Sedimentation rates ranged from 30 to 600 m/m.y. and were most commonly between 50 and 100 m/m.y., roughly three to four times the values typical for deep-sea carbonates.

The high supply of organic matter results in intense diagenetic activity. Parallel to the intensive chemical reactions directly associated with organic carbon, there are other reactions involving the dissolution and precipitation of minerals, which are an integral part of the intense diagenetic activity ultimately driven by the high productivity of overlying waters. These reactions include dissolution of biogenic carbonates and formation of calcite and dolomite, as well as other minerals such as glauconite, pyrite, and phosphate.

One of the more conspicuous discoveries during Leg 175 was the presence of several decimeter-thick dolomite layers, which were found in some cores, that could be located precisely within the holes using various logging tools. If dolomites are widespread, reinterpretation of seismic profiles, among other things, will be required. Also, the presence of dolomite layers in sediments <1 m.y. old indicates rapid development of such layers under favorable conditions.

INTRODUCTION

The Angola-Namibia upwelling system is one of the five or six great upwelling regions of the world. It extends over a considerable portion along the western margin of southern Africa, with productivity values reaching, and sometimes exceeding, 180 gC/m^2/y (Berger, 1989). The upwelling system is characterized by organic matter–rich sediments and contains an excellent record of productivity history, which, in turn, is closely tied to the regional dynamics of circulation, mixing, and upwelling of subsurface waters (Berger and Wefer, 1996b; Fig. 1).

Upwelling of cold water off southwest Africa is centered, at present, on the inner shelf and at the shelf edge. The Benguela Current flows roughly parallel to the coast, staying close to it (within ~180 km) south of 25°S. Over the Walvis Ridge, between 23° and 20°S, the Benguela Current turns to the west. At about 20°S, warm tropical water masses moving in from the north meet the cold Benguela Current and form eddies. Cold-water eddies with upwelled water contain radiolarians and diatoms and transport their load to the northern parts of the Walvis Ridge. Here, the deposits have been sampled by the Deep Sea Drilling Project (DSDP; Site 532, Hay, Sibuet, et al., 1984; Site 362, Bolli, Ryan, et al., 1978).

As reconstructed from DSDP Sites 362 and 532, the evolution of the Benguela Current during the past 10 m.y. is characterized, on the whole, by increasing rates of accumulation of organic carbon. In addition, there is evidence from changing correlations between percent carbonate, percent C_{org}, and diatom abundance, that the dynamics of the system underwent stepwise modification during the late Neogene. In this context, a distinct opal maximum in the late Pliocene to early Quaternary is of special interest. The nature of this maximum is not clear; it may be related to a migration of the polar front to its modern position, to changes in silicate content within subsurface waters, or both. The results from DSDP Sites 362 and 532 suggested that there has been a general northward migration of the Benguela Current upwelling system during the last 14 m.y. (Hay, Sibuet, et al., 1984; Diester-Haass et al., 1990). Because the shape of the South Atlantic has not changed appreciably during this time, the changes in the upwelling system must reflect large-scale changes in climate and ocean circulation.

Leg 175 focused primarily on the paleoceanographic and paleoclimatic aspects of the area. In addition, this environment provides an excellent setting for "natural experiments" in diagenesis, especially regarding the precipitation of calcite and dolomite (Baker and Kastner, 1981; Baker and Burns, 1985; Garrison et al., 1984; Murray et al., Chap. 20, this volume) and the genesis of hydrocarbons (e.g., methane; Meyers et al., Chap. 21, this volume) and phosphate (Calvert and Price, 1983). It will be of great interest to compare results with those obtained during Leg 64 in the Gulf of California (Curray, Moore, et al., 1982), during Leg 112, off Peru (Suess, von Huene, et al., 1990), and for Leg 167, off California (Lyle, Koizumi, Richter, et al., 1997).

A host of questions arise in connection with the conditions of formation of the dolomite layers and concretions. Some of the findings of Leg 175 bear on these questions, but much has to be deferred for laboratory work on shore. Here, we describe the drilling strategy and

[1]Wefer, G., Berger, W.H., Richter, C., et al., 1998. *Proc. ODP, Init. Repts.*, 175: College Station, TX (Ocean Drilling Program).
[2]Department of Earth Sciences (FB-5), University of Bremen, Postfach 330440, 28334 Bremen, Federal Republic of Germany. gwefer@allgeo.uni-bremen.de
[3]Scripps Institution of Oceanography, University of California at San Diego, Geosciences Research Division, La Jolla, CA 92093, U.S.A.
[4]Ocean Drilling Program, Texas A&M University Research Park, 1000 Discovery Drive, College Station, TX 77845, U.S.A.
[5]Shipboard Scientific Party is given in the list preceding the Table of Contents.

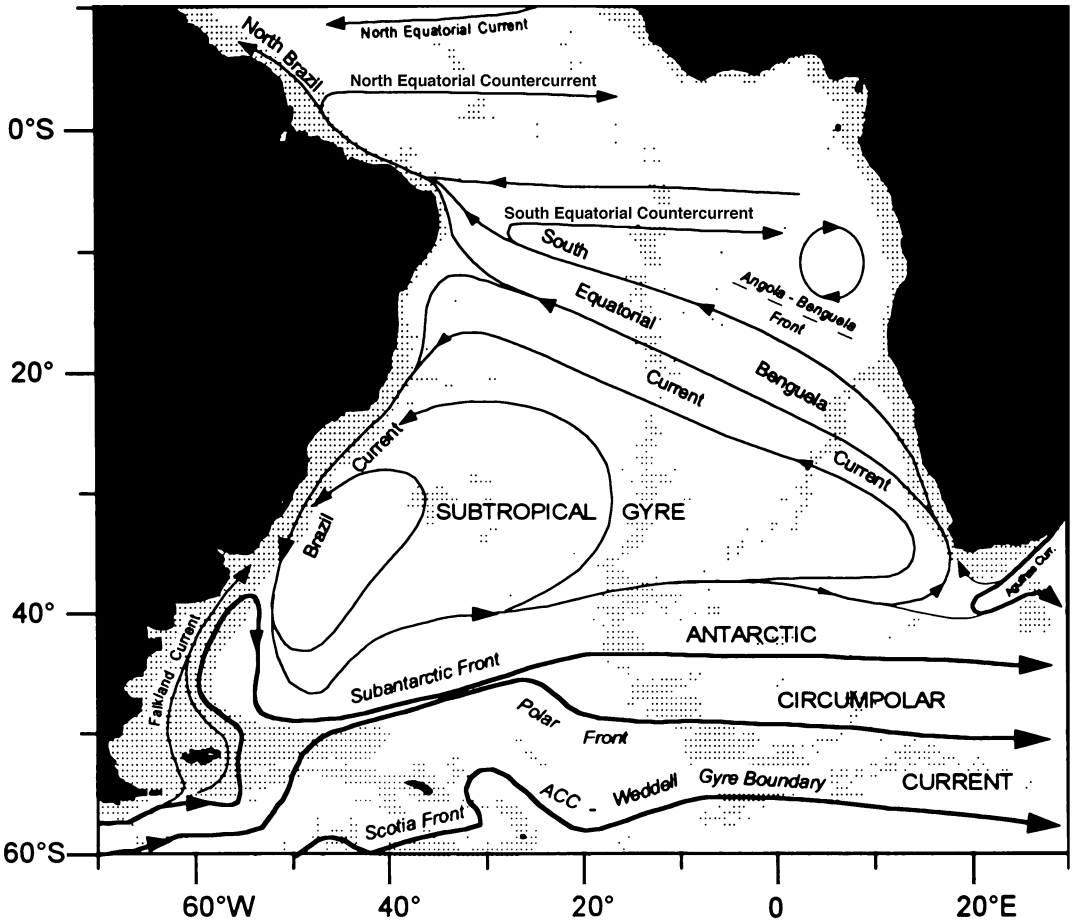

Figure 1. Schematic presentation of the large-scale, upper level geostrophic currents and fronts in the South Atlantic. After Peterson and Stramma (1991), with minor additions from several other compilations (from Berger and Wefer, 1996a).

regional setting and then turn to the presence of authigenic minerals. For this purpose, we summarize smear-slide analyses and visual core descriptions. For defining the presence of dolomite layers, the logging results are invaluable. The chemical environment is defined by the pore-water analyses. We also compare our results with those found elsewhere, with special focus on dolomite produced by early diagenesis in other depositional regimes. The layers are hard and often hinder the advanced hydraulic piston corer (APC). Drilling by extended core barrel (XCB) is necessary to penetrate the layers so that, in many cases, APC coring can then be resumed.

WORKING AREA AND SITES DRILLED

Thirteen sites were occupied during Leg 175 off the western coast of Africa, from off the mouth of the Congo River to off the Cape of Good Hope (Fig. 2). Coring was by APC from the seafloor to refusal and by XCB below refusal, where appropriate. The overall goal is to reconstruct the late Neogene history of the Benguela Current and the associated upwelling regime between 5° and 32°S.

Within this goal, the evolution of the Benguela Current system and its relationship to the onset of glacial cycles in the Northern Hemisphere is of central importance. Most of the sites show high sedimentation rates (~100 m/m.y.), offering an opportunity to develop detailed paleoceanographic records (see Berger et al., Chap. 17, this volume). The holes drilled at these sites will greatly extend and refine the partial record of the paleoceanographic and paleoclimatic changes for the late Neogene that was provided by DSDP Sites 362 and 532. Sediments are largely nannofossil clays or oozes, commonly diatomaceous, and with generally high but variable organic carbon contents (a few percent to as much as 20%).

In general, holes are shallow north of the Walvis Ridge (200 m or less) because this region has salt tectonics and is the target of active hydrocarbon exploration. On and south of the Walvis Ridge, most sites reach depths of several hundred meters below the seafloor, with the deepest site at 605 m.

As mentioned, in addition to microfossils and terrigenous materials, the sediments contain a rich assemblage of diagenetic products. There are finely disseminated euhedral dolomite crystals and other carbonates, iron sulfides of various habits (“pyrites”), and glauconites, all found in smear slides. Furthermore, up to 75-cm-thick dolomite and/or calcite layers or concretions were found in the cores or were detected with sensor tools during logging. Black, odorous, organic-rich layers are seen in places and are especially abundant at Site 1084, where they reached thicknesses of a decimeter or so. These layers also are recognizable in the logging profiles.

SEDIMENTS AND SEDIMENTATION RATES

Here, we summarize the major sediment patterns (Figs. 3–5). Rates of accumulation are typically near 10 cm/k.y. (100 m/m.y.), and vary by about a factor of 2 between sites (Fig. 3). On the whole, the hemipelagic sites to the north of the Walvis Ridge have somewhat higher rates than those south of the ridge. In hemipelagic sediments within the Quaternary record, there is a tendency for increased rates

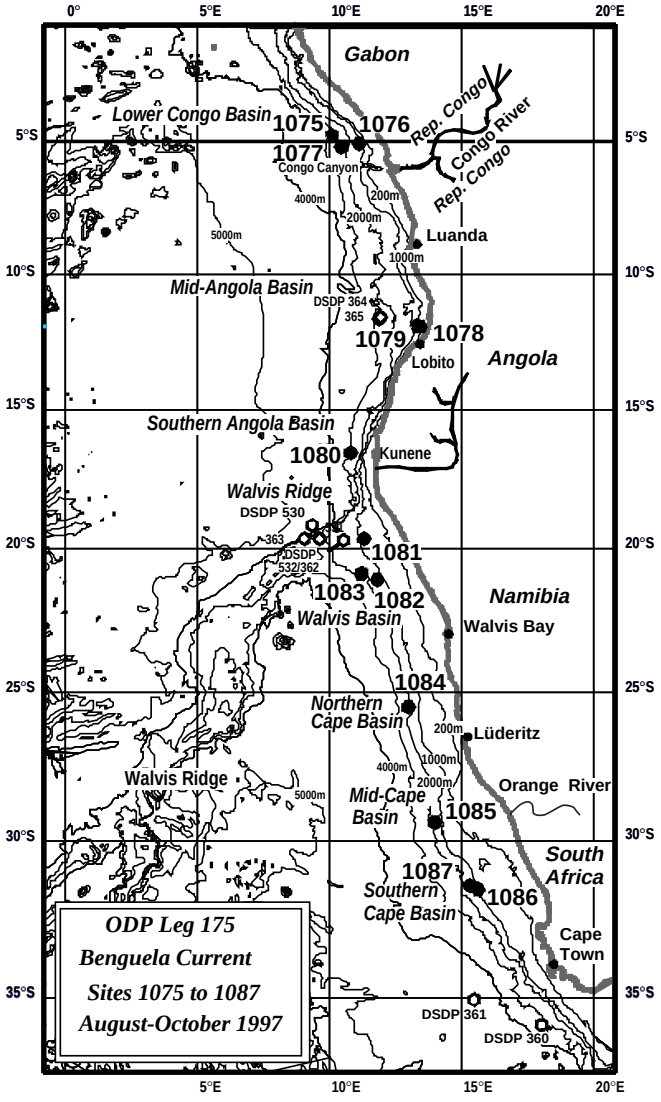

Figure 2. Overview map showing drilled sites during Leg 175 (10 August–10 October 1997, Las Palmas to Cape Town.)

with time, with maximum values in the latest Quaternary. For the pelagic sediments on the ridge and south of it, a minimum in sedimentation rate may be indicated within the early Pliocene (although this is not seen at Site 1085).

The concentration of organic carbon (Fig. 4) records a relatively modest range of variation in the sites north of the Walvis Ridge (Sites 1075–1079). Most commonly, values are between 1 and 3 wt%, with some as much as 5 wt%. There is no obvious relationship with sedimentation rates, although this has not been tested statistically. At sites south of the Walvis Ridge (Sites 1081–1085), values also are typically below 5 wt%, but reach well over 10 wt% at some sites (1082 and 1084). Noteworthy is the overall decrease in downhole percentages. Presumably, two factors are at work: (1) continued destruction of organic matter by diagenesis and (2) an increase in upwelling and productivity within the last 10 m.y. (Siesser, 1980).

The hemipelagic vs. pelagic character of sediments recovered north and south of the Walvis Ridge, respectively, is well reflected in the carbonate values (Fig. 5). At the northern sites, values tend to be low and rarely exceed 10 wt%, except at the very shallowest sites (1078 and 1079). In the southern sites, carbonate values commonly vary between 30 and 80 wt%, with the highest values in the fully pelagic sites off the Cape of Good Hope (the last two of which are not shown in Figs. 3–5). At the northern sites, a maximum carbonate event may be indicated, centered near 0.8 to 0.9 Ma. In the southern sites, a carbonate minimum appears near 1.9 Ma, at the beginning of the Quaternary record.

The patterns may be grouped into (1) Congo Fan sites (1075–1077), (2) Angola (Lobito) sites (1078 and 1079), (3) Walvis sites ([Walvis Ridge and Walvis Basin] 362, 363, and 530–532, and 1081–1083), Namibia (Lüderitz) site (1084), and South African sites (360, 361, and 1085–1087), based on carbonate and organic matter contents and sediment composition, as well as other components (opal and terrigenous contents; Fig. 6)

The Congo Fan sites (1075, 1076, and 1077) feature hemipelagic muds, typically classified as greenish gray and olive-gray diatomaceous clay, which is nannofossil bearing in places. Carbonate contents are low, especially in sediments older than 1 Ma. Sedimentation rates are close to 100 m/m.y. and typically vary by a factor of 2 around that value. Organic carbon content varies mostly between 2 and 3 wt%. Distance from the coast is reflected in the amount of reworked material and in sedimentation rates, with Site 1076 being closest to the coast and Site 1075 being the most distal. Surprisingly, we found no turbidites intercalated into the sequences. Presumably, coarse sediments moving within the deeply incised Congo Canyon are carried far into the deep Angola Basin (Jansen et al., 1984). At the sites drilled, only fine materials not confined to the canyon are delivered, perhaps from riverine plumes, through sedimentation by aggregates and in fecal pellets.

The Lobito sites (1078 and 1079), on the upper continental slope off Angola, are strongly influenced by the influx of terrigenous material. They feature hemipelagic muds typically classified as olive-gray silty clay with varying amounts of nannofossils and foraminifers. Rapid uplift of the coast and canyon cutting into the uplifted terraces provide much of the terrigenous supply, which drives up sedimentation rates (Fig. 3). Considering the dilution effect of the terrigenous silt and clay, the organic content is surprisingly high, with values between 2 and 5% (Fig. 4). High nutrient supply associated with the Angola Dome upwelling, as well as coastal mixing, combine to provide for high productivity in this area.

Site 1080, off the Kunene River, was drilled only to 52 meters below seafloor (mbsf) when drilling was halted by hard dolomite. The sediment is diatomaceous hemipelagic mud, classified as greenish gray and olive-gray diatom-bearing and diatom-rich silty clay. Sedimentation rates are near 100 m/m.y., but the upper Quaternary record is missing.

The Walvis sites ([Walvis Ridge and Walvis Basin] 1081, 1082, and 1083) show a strong influence from high productivity in the coastal ocean. Sediments are intermediate between hemipelagic mud and pelagic ooze and are typically classified as olive-gray nannofossil-rich clay or ooze with or without a strong admixture of diatoms. In sections with very high carbonate content (e.g., Site 1083), the color is pale yellow or pale olive. Alternations of sediment types are common and produce color cycles. The opaline component is especially high in the upper Pliocene and lower Pleistocene sediments.

The Lüderitz site (1084), located between Lüderitz Bay and Walvis Bay, represents the extreme among all sites regarding upwelling and productivity. Sediments are intermediate between hemipelagic mud and pelagic ooze and are typically classified as nannofossil-rich diatomaceous clay, diatomaceous clay, and nannofossil clay or ooze. On the whole, sedimentation rates well exceed 100 m/m.y., but not so much from unusually high delivery of terrigenous mud as from the high supply of nannofossils, diatoms, and organic matter. Black layers extremely rich in organic carbon are common at this site beginning in the upper Pliocene, and they increase in abundance toward the present. As at the Walvis sites, diatom abundance reaches a maximum in upper Pliocene and lower Pleistocene sediments.

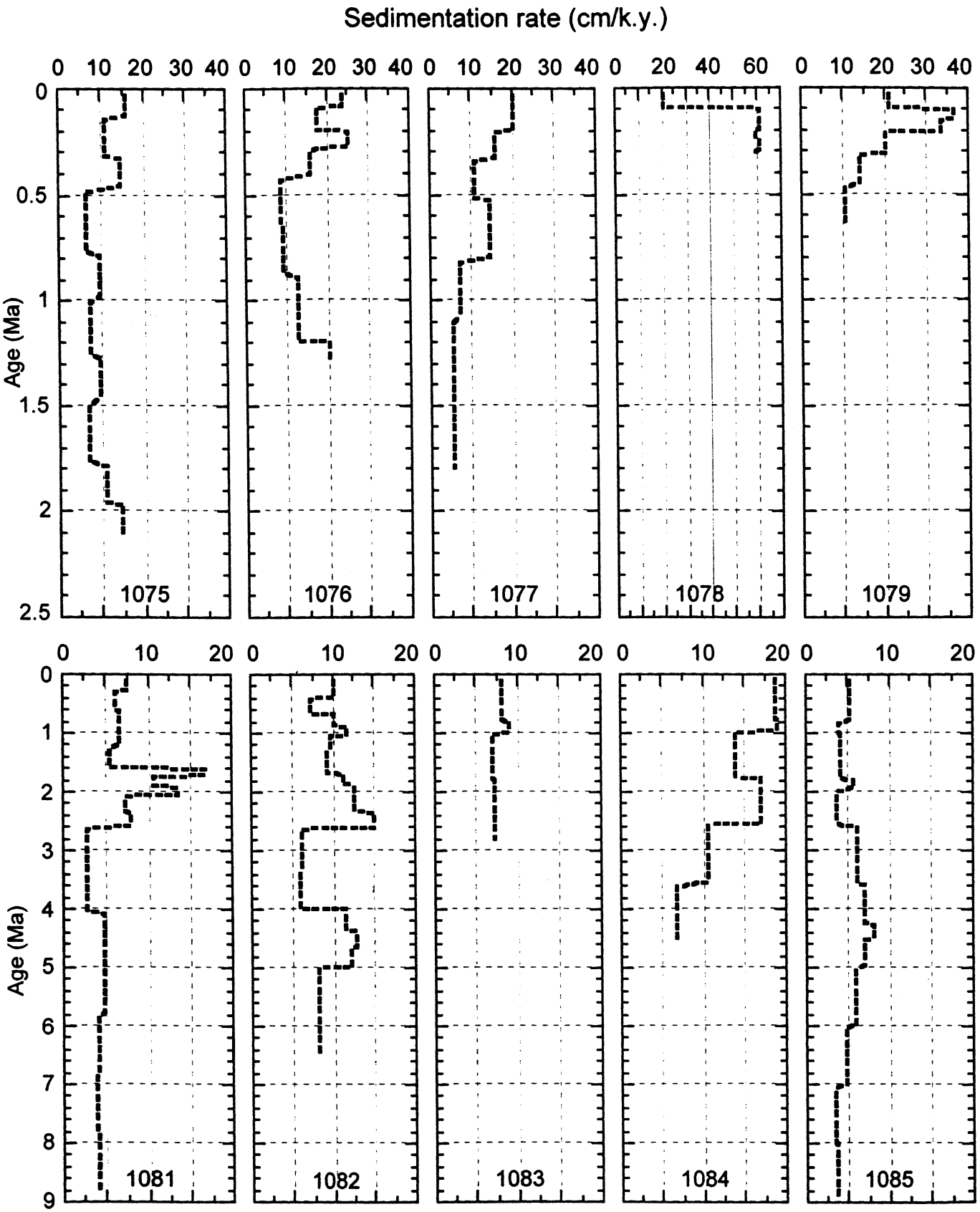

Figure 3. Patterns of sedimentation rates at Sites 1075–1085, drilled during Leg 175, based on biostratigraphy and paleomagnetic reversals (see individual site chapters, this volume).

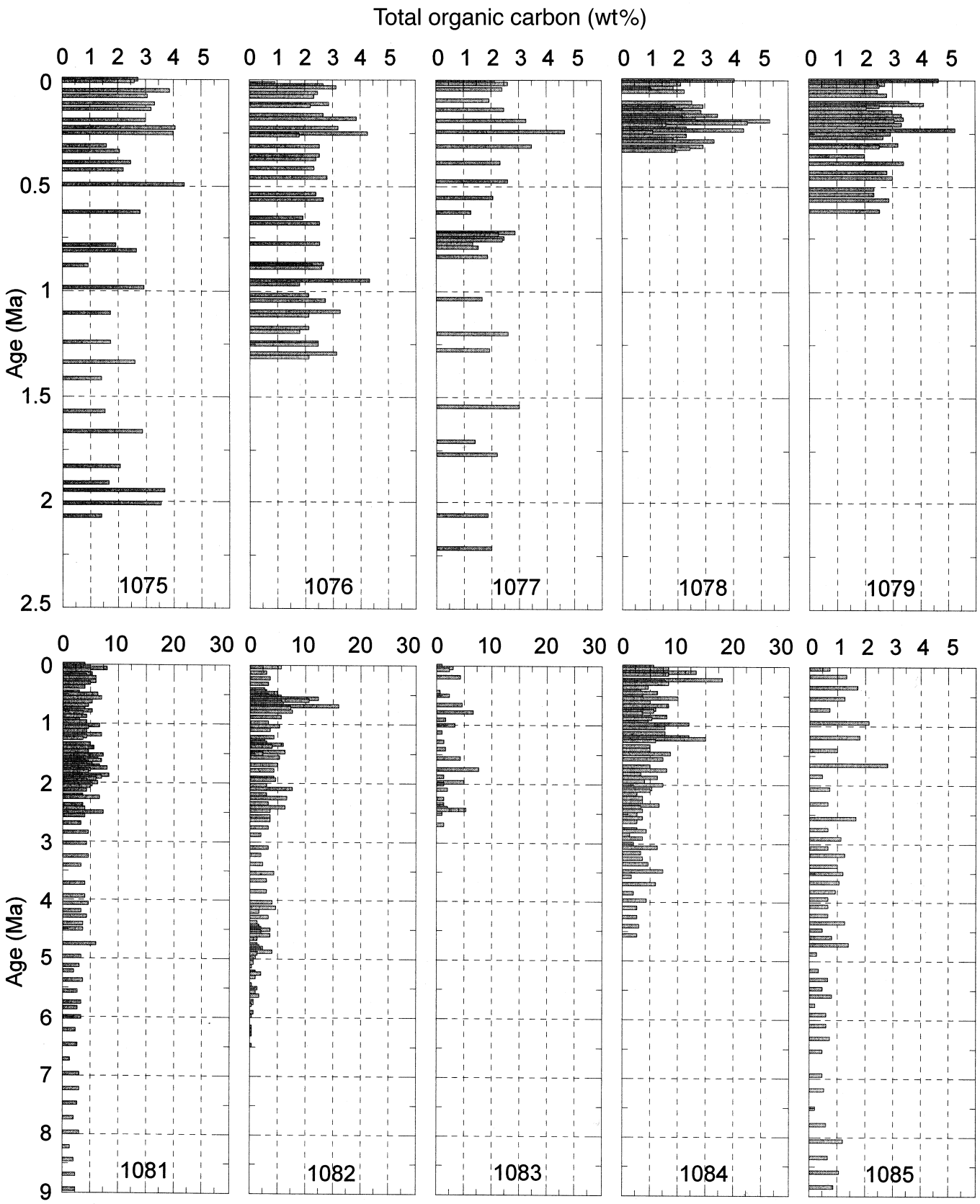

Figure 4. Patterns of organic carbon abundance at Sites 1075–1085, drilled during Leg 175.

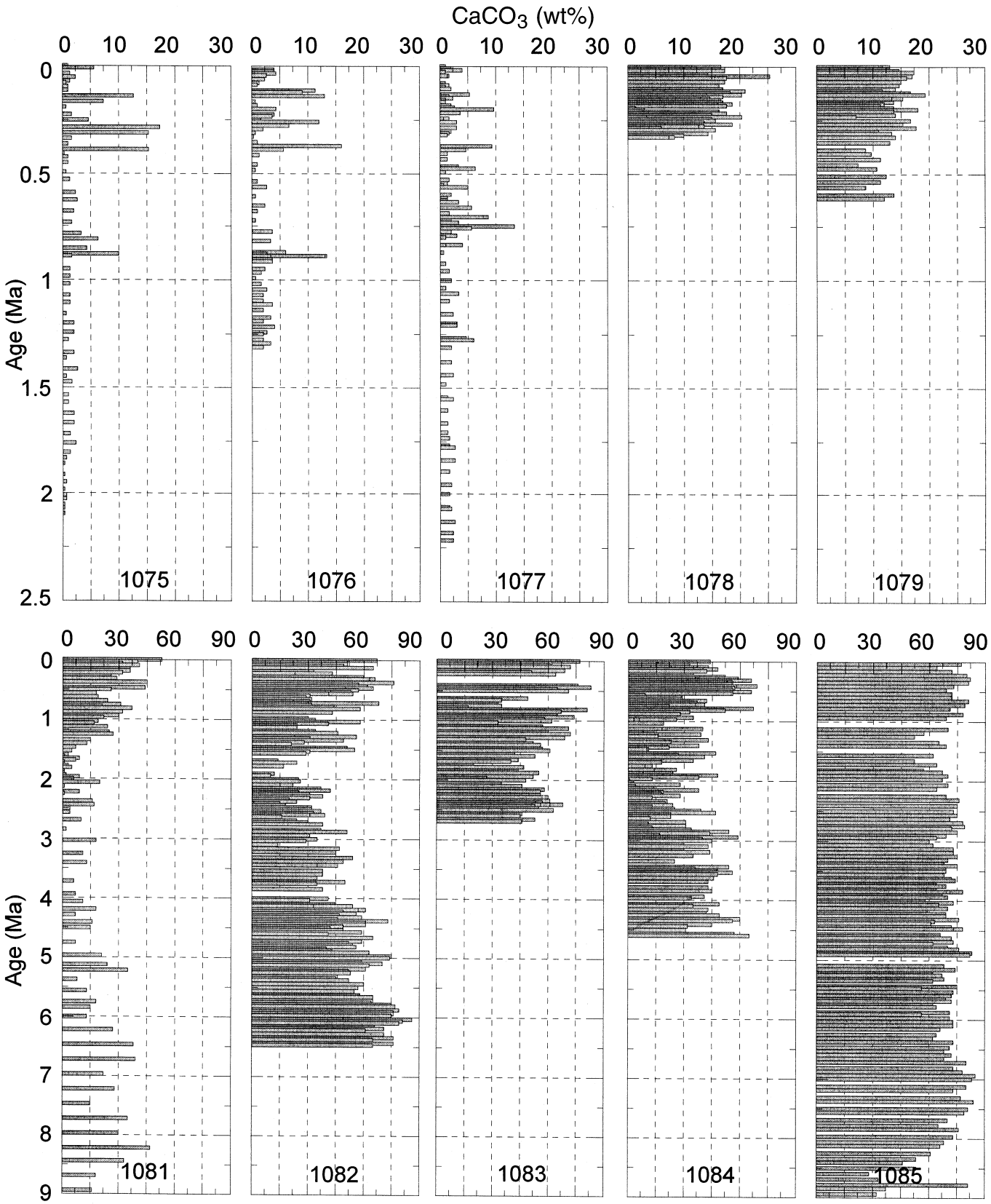

Figure 5. Patterns of carbonate abundance at Sites 1075–1085, drilled during Leg 175.

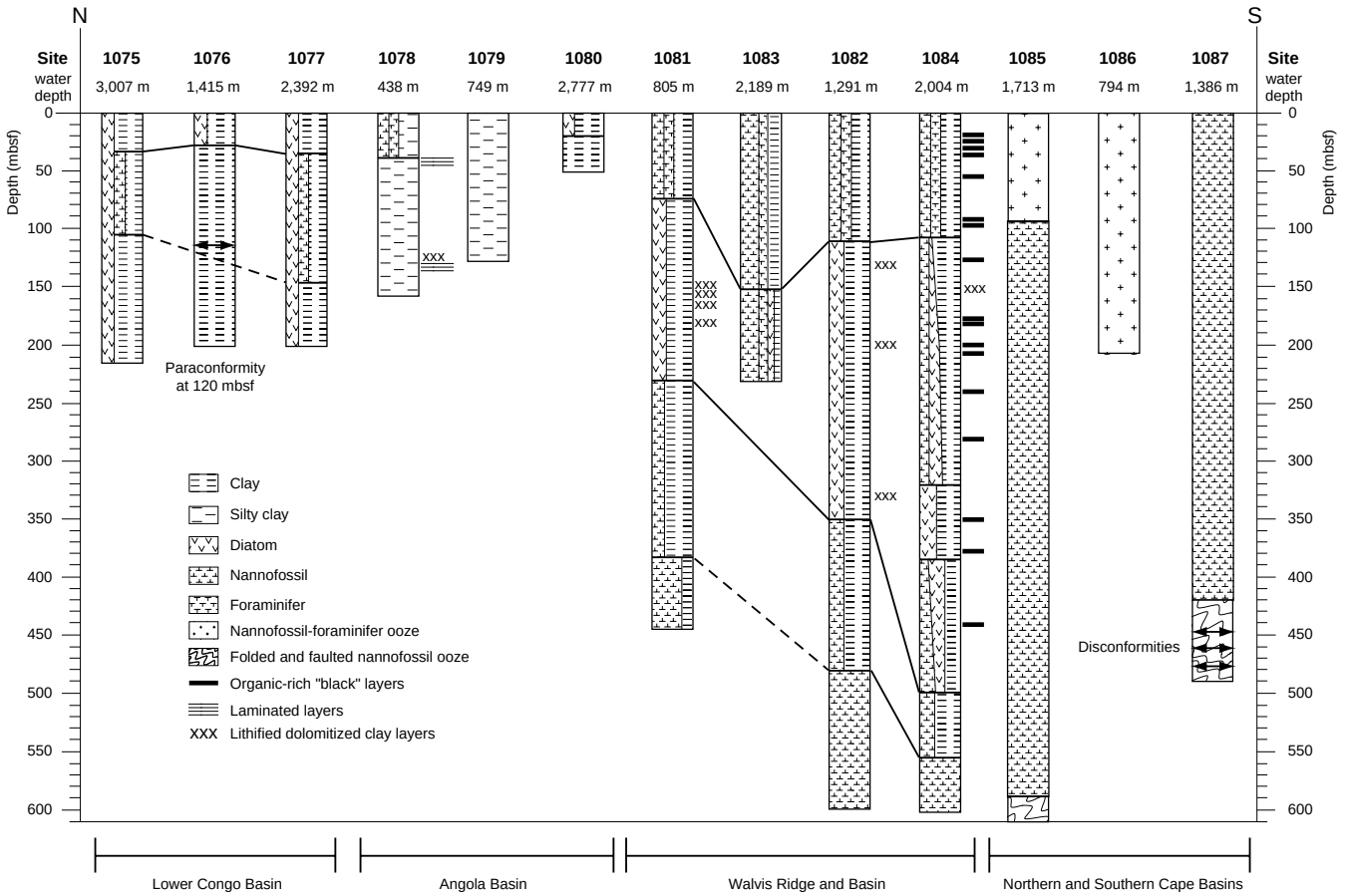

Figure 6. Facies patterns at sites drilled during Leg 175 (from Pufahl et al., Chap. 18, this volume).

The South African sites (1085, 1086, and 1087) show, on the whole, pelagic sedimentation. Sediments are typically classified as foraminifer-rich nannofossil ooze, with variants on this theme, depending on clay, diatom, and foraminifer content. Carbonate content is high, whereas organic carbon content is modest (although higher than average for pelagic carbonates). Sedimentation rates vary mostly between 20 and 60 m/m.y., which is about twice the rate for pelagic deep-sea calcareous ooze. At these sites, drilled to a maximum depth of 604 m in places, the oldest sediments were recovered. At Site 1087, a continuous record (apparently) dates back to the middle Miocene, whereas older sediments (early Miocene, Oligocene, and Eocene) are present but separated by hiatuses.

LOGGING RESULTS

Logging proved extremely useful in pursuing the goals of Leg 175 and delivered a number of entirely unexpected insights. A large number of sensors were available, which produced many vitally important details regarding conditions of sedimentation at the logged sites. In addition, the profiles were very useful in correlating cores with in situ sequences. Hole conditions were generally quite good, and only the results from the sites drilled into pelagic carbonates (Sites 1085 and 1087) were less than optimal.

Most holes were logged four times. The first tool string (seismostratigraphy) included the spectral gamma-ray (NGT), sonic, electrical induction, and temperature (TLT) sondes. This combination is useful for describing lithology, sedimentary fabric, and degree of lithification. The second tool string (lithoporosity) included the NGT, neutron porosity, gamma density, and TLT sondes. The third tool string (Formation MicroScanner [FMS], 2 passes) included the NGT, inclinometry, and FMS sondes. The FMS tool string produces high-resolution electrical resistivity images of the borehole wall, which can be used to study the structure of bedding, diagenetic features, hiatus, and cyclicity recorded in the sediments. The fourth tool string (geological high-sensitivity magnetic tool [GHMT]) included the NGT, magnetic susceptibility, and vertical component magnetometer sondes. The GHMT provides continuous measurements of magnetic susceptibility and the vertical component of the total magnetic field. This latter measurement provides a magnetic reversal stratigraphy, provided the magnetization of the sediments is sufficiently strong.

As an example of the importance of logging in defining sediment sequences, we show results from Site 1081 (Fig. 6). The width of the hole is measured by the caliper log (first column); it shows that the hole is in good condition. Below 300 m, the width is almost precisely 10 in throughout; above this level, the hole is expanded at the ends of piston core sections (at 9.5-m intervals). With the exception of a few disturbed places, these expansions are minor (typically 1–2 in).

Commonly (but not invariably) there is good correspondence between lithology and the physical properties recorded by logging. At Site 1081, for example, a notable change occurs near 190 mbsf in average gamma-ray intensity, resistivity, density, and magnetic susceptibility (Fig. 7). This change may be associated with the facies boundary 1b/1c, from black and dark olive-gray diatom-rich clay to olive and olive-gray nannofossil-rich clay. The transition from the diatom-rich nannofossil-poor unit above to the nannofossil-rich diatom-poor unit below is gradational; it also marks a decrease in organic carbon content. The sense of change in resistivity and density is readily un-

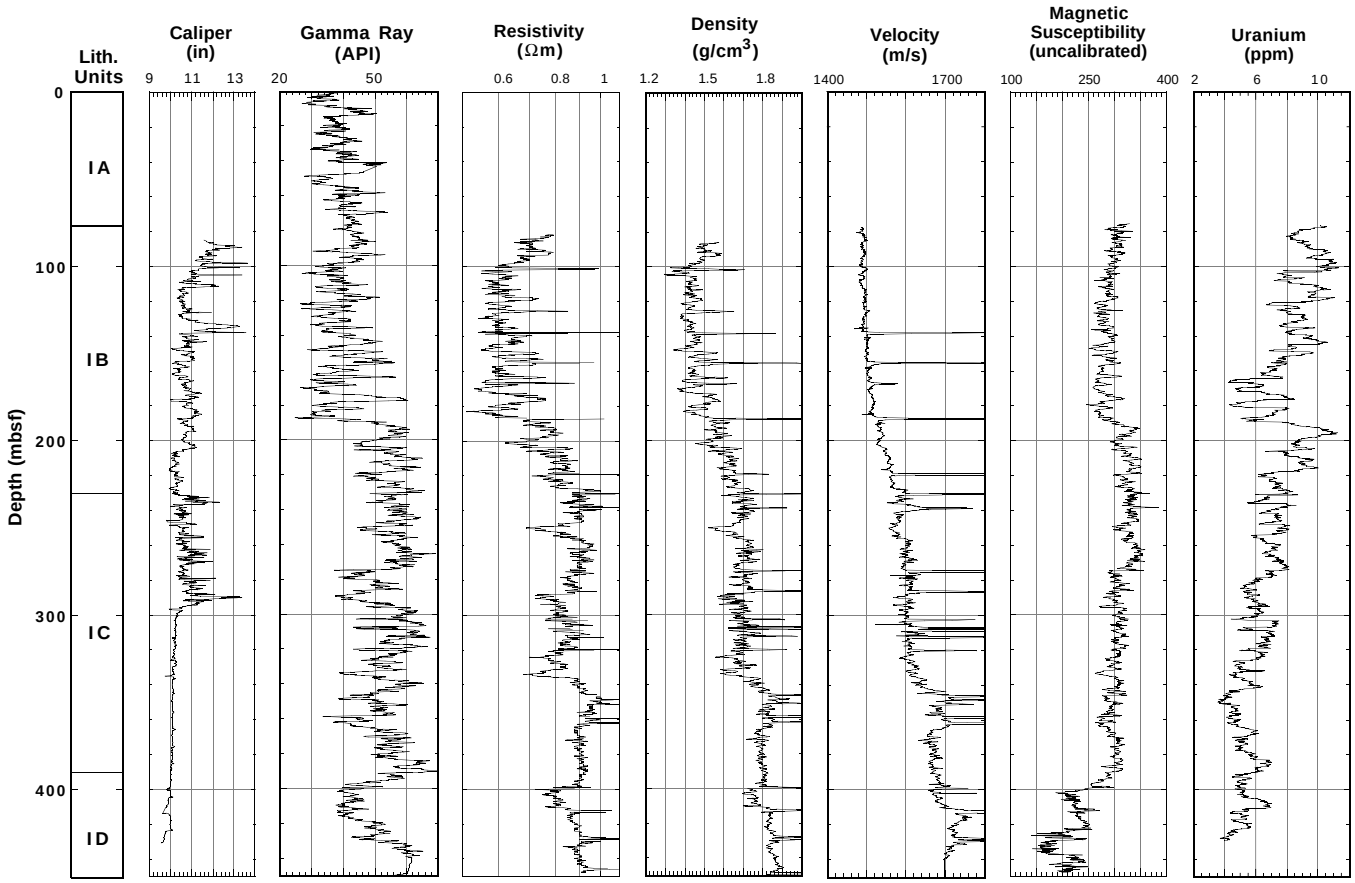

Figure 7. Downhole logs of caliper, natural gamma ray, velocity, and density from Hole 1081A.

derstood. The other parameters (gamma ray, susceptibility, and uranium content) are less readily visualized in their dependency on facies. The overall trend in uranium may reflect an overall increase in organic matter content through time. The overall downhole increases in density and sonic velocity reflect compaction and lithification.

Of special interest are the distinct spikes in resistivity, density, and sound velocity, which occur throughout the logged profiles and are strictly correlated with one another. These spikes are interpreted as discrete layers of dolomite and calcite, or dolomite-cemented and calcite-cemented clay. There are 25 such layers at Site 1081. Because of their high resistivity, these layers are readily identified by FMS; thus, their positions and thicknesses can be accurately determined. Of these 25 layers, only four were recovered in the cores, and 11 were sampled with the core catcher (Fig. 8).

DOLOMITIC LAYERS AND DISSEMINATED RHOMBS

As previously mentioned, much of what we infer about the distribution of dolomitic layers is based on logging results. Cores and core catchers did contain samples from some of the layers seen in the logging profiles, but many of these samples consisted of small fragments. In addition to being present in solid layers, dolomite and calcite are also present as concretions and as disseminated small crystals.

Dolomite is commonly present together with phosphorite; presumably, the precipitation of both is stimulated by the effects of high productivity. Apparently, productivity must be sufficiently high to generate a favorable environment, but other factors also are important. Many questions are open at this point:

1. Why are dolomite layers present in the Guaymas Basin (Gulf of California, Leg 75), in the coastal upwelling area off Peru (Leg 112) and California (Leg 167), and in the Benguela upwelling system off Namibia (Leg 175), but absent in the equatorial upwelling regions in the Pacific (Leg 138), Atlantic (Leg 108), off southwest Africa (Leg 108), and off Oman (Leg 117)?
2. What determines the exact stratigraphic position of dolomite layers in the host sediment?
3. What are the chemical conditions under which precipitation takes place, and what are the chemical reactions taking place?
4. Do disseminated dolomite crystals coalesce into larger concretions? Do concretions coalesce in layers?
5. Can one recognize the dolomite layers in seismic profiles?

These questions cannot be properly addressed by shipboard results. Here, we can only give some preliminary discussions. Whether disseminated dolomite (or calcite) crystals are associated with dolomite layers can be checked to some extent with smear-slide data. It is reported that dolomite crystals can form during early diagenesis in organic-rich sediments already a few centimeters or decimeters below the sediment surface (e.g., Shimmield and Price, 1984; Suess, von Huene, et al., 1988, Leg 112). However, isotopic analyses showed that most of the disseminated dolomite crystals form later at greater depths in the sediment. Presumably, the more conspicuous layers and

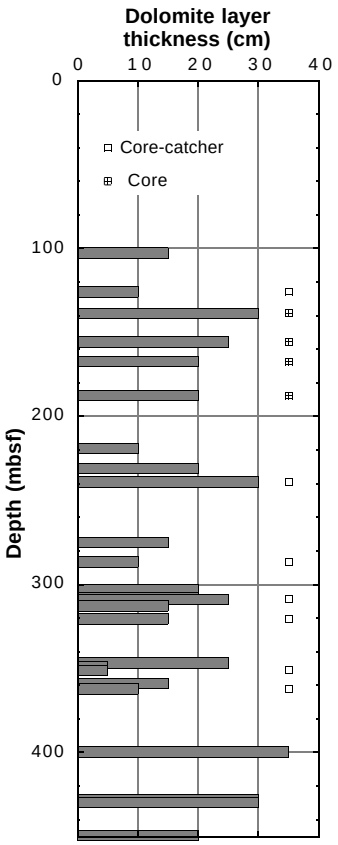

Figure 8. Thickness of dolomite layers as a function of depth in hole, as seen in the FMS profiles and other logs at Site 1081.

concretions form within unconsolidated sediments by precipitation and replacement in depths of tens to hundreds of meters below the seafloor.

The abundance patterns of dolomite rhombs at our sites show that rhombs are much more common at some sites than at others (Fig. 9; the categories from 1 to 5 are semi-quantitative and denote trace, rare, frequent, common, and abundant). Sites near the coast (Site 1076 off the Congo, Sites 1078 and 1079 off Lobita, and Sites 1081 and 1082 on the slope of the Walvis Basin) seem to show the higher values. There seems to be no obvious relationship to the presence of opal or organic matter or carbonate content.

Carbonate particles show a pattern that is entirely different from that of the dolomite rhombs (Fig. 10). They are most abundant in the sites far from the coast (1082–1085), more or less independently of the composition of the sediment and of organic matter content. Except for Site 1083, there seems to be a minimum near 2.5 Ma at the sites south of the Walvis Ridge.

A comparison of Figures 9 and 10 suggests that dolomite rhombs and carbonate particles may be mutually exclusive to some degree. This may indicate geochemical preferences for dolomite formation, or it may (at least in part) reflect a difficulty in identifying rhombs among abundant carbonate particles.

The patterns do not readily lead to hypotheses about the formation of dolomite. At the first three sites, off the Congo, no dolomite concretions or layer were found. They were first encountered in the organic-rich sediments off Angola (Site 1078). This site is strongly characterized by terrigenous influx; sediments are carbonate rich and contain little diatom debris. Several dolomite layers ~3 to 7 cm thick were found in Sections 175-1078C-13H-1 (111.7 m), 15X-3 (131.4 mbsf), and 175-1078D-10H-3 (82.9 mbsf). Smear-slide determinations show trace (0–120 m) and trace to frequent (135–140 mbsf) abundances (Fig. 9). For carbonate, there is a modest maximum between 112 and 130 mbsf (Fig. 10). Again, there is no evidence for an association among these three abundance observations. No dolomite layers were found at Site 1079; possibly, the holes drilled were too shallow, although at the adjacent Sites 1078 and 1080, dolomite was detected at depths of <100 m. These findings demonstrate that dolomite formed within the last million years.

The presence of a hard dolomite layer at rather shallow depths in the two holes drilled at Site 1080 (52 and 38 mbsf, respectively) was one reason drilling was terminated at this site; another was the fact that the late Quaternary record is largely missing. Dolomite rhombs (not shown in Fig. 9) were seen in trace abundances between 0 and 26 mbsf and near 35 mbsf. Carbonate was frequent near 20 mbsf and rare near 35 mbsf.

Dolomite layers, as previously mentioned, were found to be quite abundant at Site 1081, mainly on the basis of logging, but also verified through samples in cores and in core catchers (Fig. 8). It should be possible by comparison with Ocean Drilling Program (ODP) Sites 1082 and 1083 and DSDP Sites 532 (1331 m) and 362 (1325 m) to study dolomite formation under similar conditions, but with slightly different levels of productivity and interstitial water composition. Although the comparison sites are seaward of the upwelling center, they show higher organic carbon content because of transport of upwelled water to these locations by the Benguela Current and its filaments. As far as abundances at Site 1081, there is no evidence that dolomite layers and dolomite rhombs have a tendency to be present together; the opposite is more likely (Fig. 11A). Also, where carbonate is recorded in smear slides, dolomite layers are no more likely (perhaps less likely) to be found than elsewhere. Similar observations may be made at Site 1082 (Fig. 11B). In fact, dolomite rhombs and dolomite layers were never reported together at any depths. Regarding the general pattern, the presence of diatoms, foraminifers, or nannofossils allows no statement regarding the likelihood of finding dolomites at either site.

At Site 1083, located only 25 km to the northwest of Site 1082, but at a greater water depth (2200 m), no dolomite was found. Carbonate contents are rather high (50 to 70 wt%) and C_{org} values are distinctly lower than those at Site 1082.

At Site 1084, the extreme-productivity site, sulfate is completely consumed at <6 mbsf. Many lithified carbonate layers were identified in the logging profiles based on density, velocity, and resistivity. In Hole 1084A, a thick hard layer (apparently underlying soft nannofossil ooze) was hit with the APC at ~120 mbsf. Lithified layers do not seem to be present at all holes at the same depth, suggesting isolated concretions perhaps arranged in horizons (as familiar from outcrops on land).

No dolomite layers or concretions were seen at Site 1085. Disseminated dolomites are described in places (in the smear-slide analyses), especially in sediments older than Pliocene in age.

CONDITIONS FOR DOLOMITE FORMATION

From the above comparisons of patterns among dolomite rhombs, carbonate particles, and lithified layers, and from the patterns of sedimentation, it is clear that although dolomite formation is somehow tied to high productivity, the important details remain unsolved when using only this field evidence. Presumably, the reduction of sulfate and the concomitant increase in alkalinity are crucial factors (Baker and Kastner, 1981; Compton, 1988; Kastner et al., 1990). Disseminated dolomite can be present at very shallow depths below the seafloor (e.g., Shimmield and Price, 1984; Kulm et al., 1984; Suess, von Huene, et al., 1988), presumably reflecting highly reducing micro-

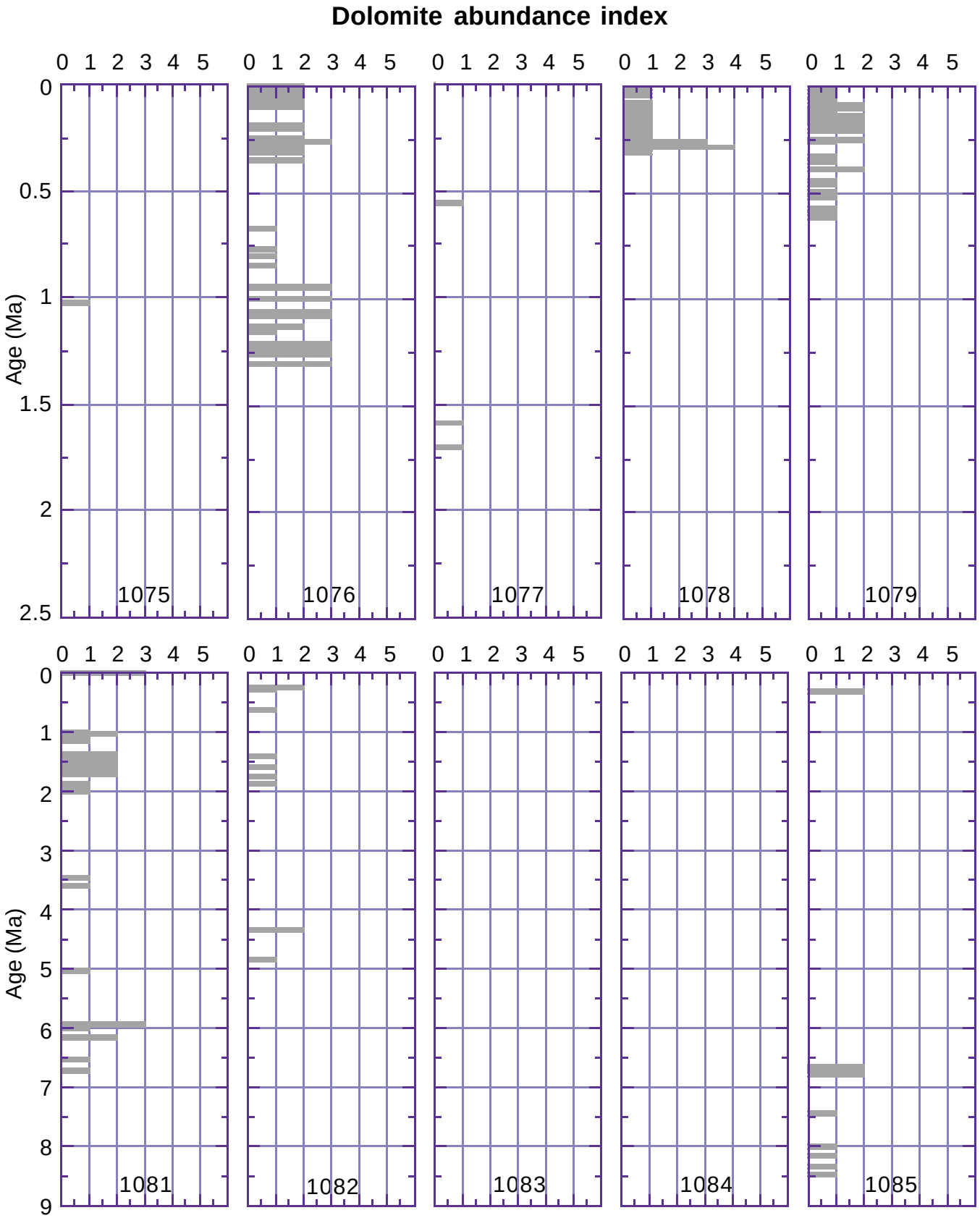

Figure 9. Abundance pattern of disseminated dolomite rhombs at Leg 175 Sites 1075–1085, based on smear-slide analysis (see individual site chapters, this volume).Values 1–5 denote the categories trace, rare, frequent, common, and abundant, respectively.

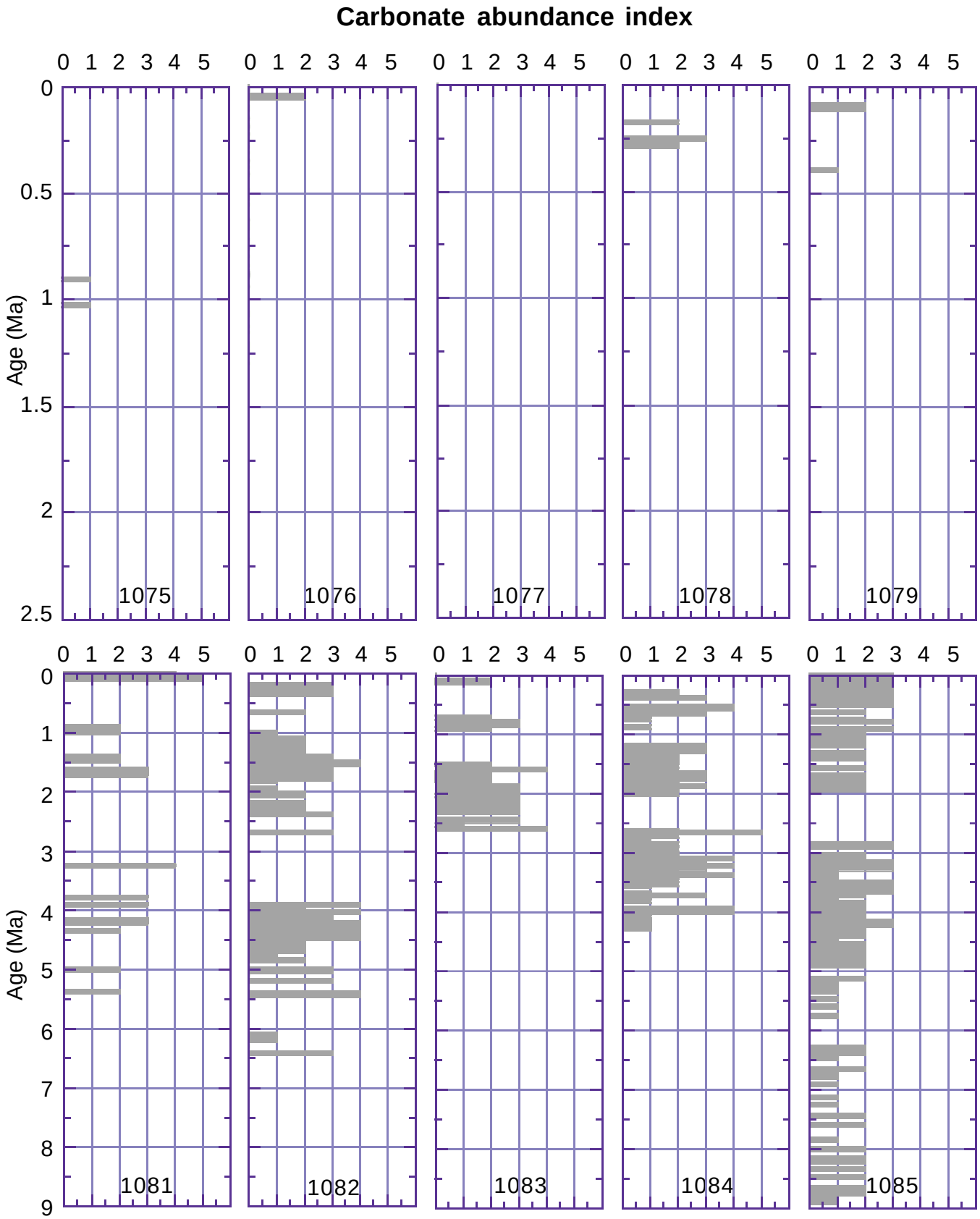

Figure 10. Abundance pattern of carbonate particles in cores from Sites 1075–1085, based on smear-slide analysis (see individual site chapters, this volume). Categories 1–5 are the same as in Figure 9.

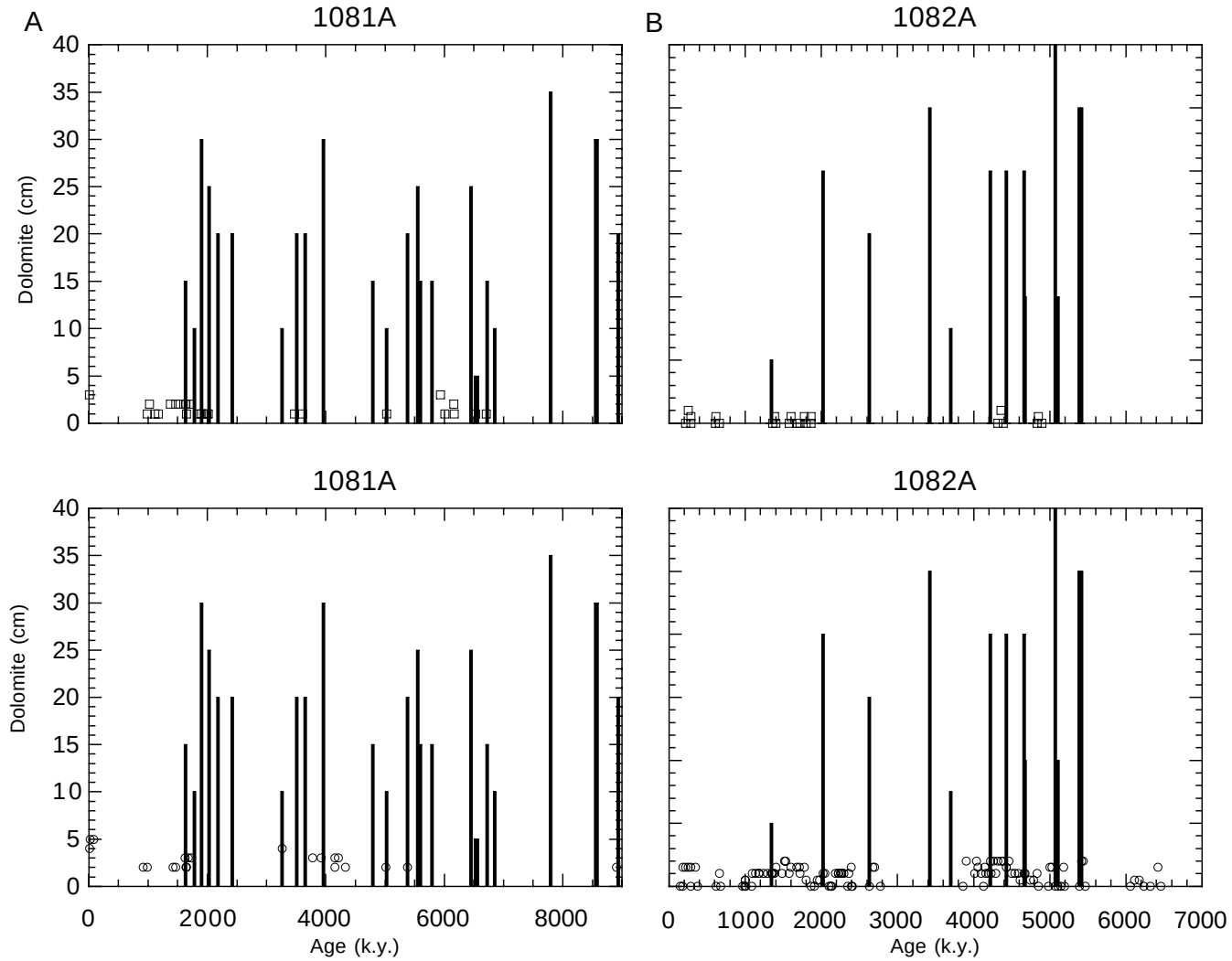

Figure 11. Abundance patterns of dolomite rhombs and carbonate particles (from smear-slide analyses; categories 1–5 are the same as in Figure 9) at (**A**) Hole 1081A and (**B**) Hole 1082A, together with dolomite layers seen in logging profiles (values denote thickness of dolomite layers). Shaded bars = thickness of dolomite layers (cm); open squares = dolomite rhombs; open circles = carbonate particles.

environments featuring low sulfate and high alkalinity. It is possible that the presence of clay-sized detrital dolomite plays a role in some of these abundance patterns and provides seeds for growth. The availability of dissolved iron might play a similar role in providing the precipitation of seed crystals (cf. Henderson et al., 1984). Dissolved Mg is available for dolomitization from diffusion from overlying sea water (Baker and Burns, 1985; Compton and Siever, 1986). Other sources of Mg are thought to be of minor importance for dolomite formation in continental margin sediments (Baker and Burns, 1985). Removal of calcium from solution (e.g., by precipitation of authigenic calcite in a zone of high alkalinity) might precondition solutions for precipitation of increased proportions of Mg-rich carbonate as a precursor for dolomite (Burns et al., 1988). It is likely that a number of factors have to be balanced precisely to provide the correct environment for dolomite formation, beginning with a sedimentation rate high enough to preserve organic carbon below the sediment/water interface, but low enough to prevent excessive dilution of the reactants (e.g., Baker and Burns, 1985).

At Leg 175 sites, we commonly observed dual depletion of Ca^{2+} and Mg^{2+} from the interstitial waters through the same depth range that high alkalinities are generated by degradation of organic matter (Murray et al., Chap. 20, this volume). These pore-water profiles strongly suggest that dolomite is actively precipitating in the uppermost 50–70 mbsf of the sediment column and speaks to the intimate associations between organic matter remineralization, the dissolution of biogenic calcite, and the formation of diagenetic dolomite (Murray et al., Chap. 20, this volume).

SEISMIC PROFILING AND LITHIFIED LAYERS

The question naturally arises whether the dolomite layers and similar lithified beds are recognizable in seismic profiles. Judging from the data available for Site 1082, the answer is ambiguous: some are, some are not, and many reflectors seen are not from lithified layers (Fig. 12). Reflectors arise where there are sudden changes in density or velocity, or both, and such changes can be provided by different changes in sedimentary facies. Dolomitic intervals represent thin layers with regard to the seismic wavelengths. For this conditions, reflection amplitudes are not directly proportional to the change in acoustic impedance but depend on geometry and continuity of the layers. Some of the dolomitic layers seem clearly recognizable as

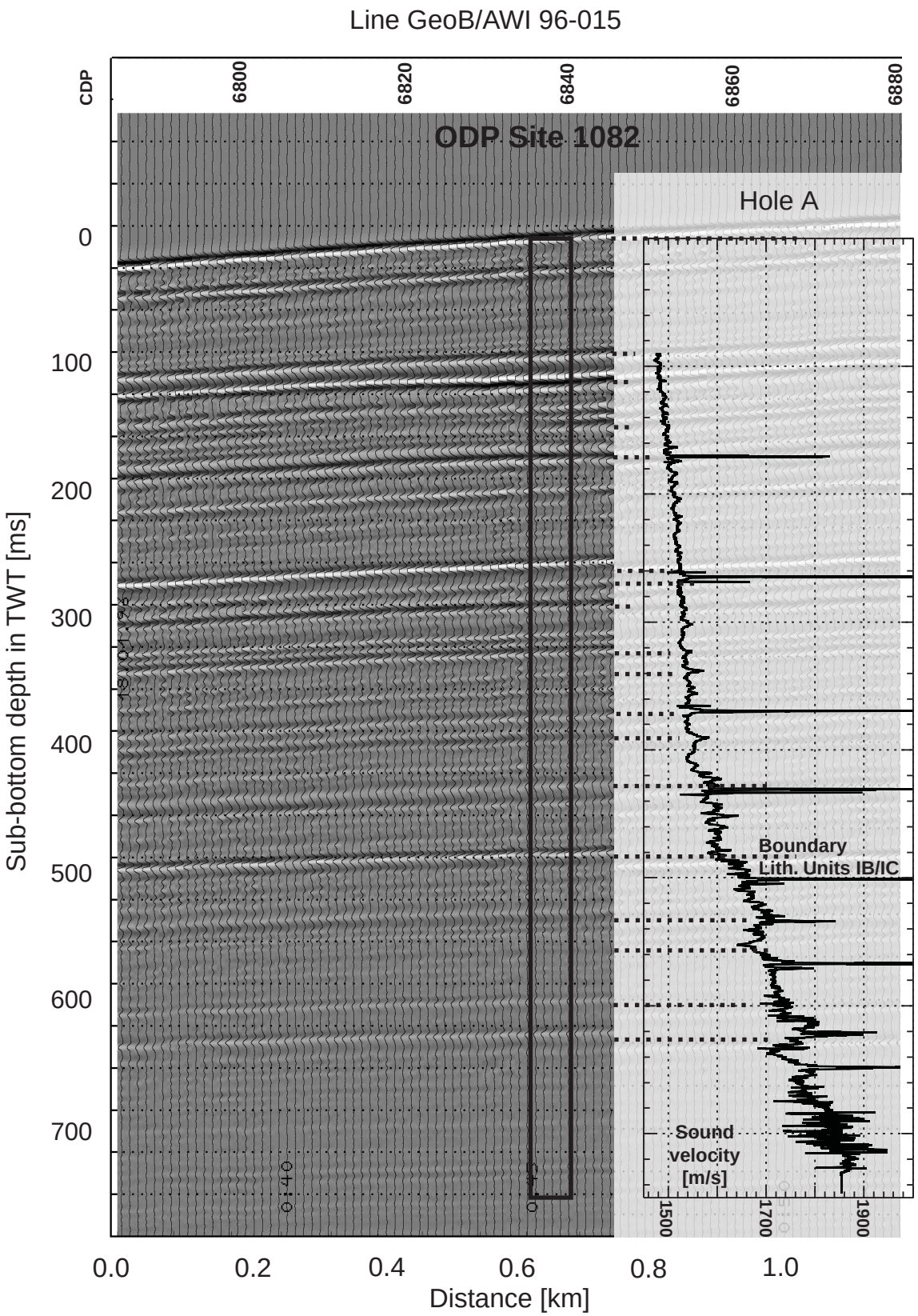

Figure 12. Comparison of a seismic profile across Site 1082 with the position of lithified layers, as seen in the sound velocity profile of downhole logging. Selected reflectors can be correlated with local extremes in the velocity log (dashed lines) and may indicate the presence of lithified intervals or dolomite clays.

continuous, high-amplitude reflectors in the seismic profiles. However, a dependency on layer thickness (reconstructed from logging data) could not be observed. Also, it is surprising that the band of lithified layers between 300 and 320 mbsf on the Walvis Ridges is not associated with more pronounced amplitudes.

Phosphorite

We expected to see more phosphorite minerals than we found, based on previous reports of phosphorite abundance off southwest Africa. During Leg 175, phosphorites were noted only in sediments from the Congo Fan sites, as well as in the two southernmost sites (1086 and 1087). In both cases phosphorites may not be forming in situ, but rather were brought in from the shelf. Phosphorites are abundant on the shelf of Namibia, where sporadic winnowing of deposits is an important factor in concentrating the material (Calvert and Price, 1983).

It is unlikely that phosphatic minerals are absent in most of the sites drilled during Leg 175. The intensity of sulfate reduction in many of these sites indicates active oxidation of organic matter, which releases phosphorus. At every site drilled during Leg 175, concentrations of dissolved phosphate increase through the uppermost 50 mbsf, which is the zone of intense organic matter remineralization (Murray et al., Chap. 20, this volume). Below these relatively shallow maxima in dissolved phosphate, the concentration dramatically decreases, indicating the precipitation of authigenic phosphate minerals. The finely disseminated apatite is physically difficult to observe.

Authigenic Iron Sulfides

Pyrite (and other iron sulfides) were observed in smear slides at all sites, but most commonly at Sites 1075 and 1076 on the Congo Fan (Fig. 13). Because organic matter (for the reduction of sulfate) is not particularly abundant here compared with other sites (Fig. 4), we assume that the availability of iron is the decisive factor in generating high abundances of pyrite at these sites. Some of this iron may reach the site of deposition bound within clay minerals; much may be in the form of iron (hydr)oxide coatings, or flocs. Low iron sulfide abundances are typical for sites (e.g., 1083 and 1085) where organic matter contents are low, carbonate values are high, and influx of terrigenous sediments is reduced.

The growth of iron sulfide aggregates proceeds from finely disseminated iron monosulfides (Siesser, 1978), which take up sulfur to form microscopic crystals of pyrite, marcasite, and other sulfides. In the uppermost cores of a hole, the microscopic crystals within aggregates smear over some distance when the core is cut into sections, producing long streaks emanating from a pocket source (e.g., a burrow). Deeper in the holes, pyrite is present as small nodules and tubes. At Site 1085, the transitions are remarkably well expressed from disseminated pyrite to isolated silt-sized and sand-sized grains (starting at ~130 mbsf) and from grains to nodules as much as 1 cm in diameter (starting at ~430 mbsf). At Site 1086 (with a facies similar to that at Site 1085 but with even higher carbonate content), small, fine sand-sized pyrite grains are present below ~150 mbsf.

Large pyrite concretions were found at Site 1087, the southernmost site and the one with the highest carbonate content and with comparatively low sedimentation rates. Sand-sized pyrite grains are common throughout the sediment column. In Core 175-1087C-50X (453.5 mbsf) an ~3-cm-thick pyritic aggregate is present, as well as several other centimeter-sized pieces. Pyrite aggregates at this horizon are rimmed with iron (hydr)oxides, which suggests a return to a more oxidizing environment after pyrite formation. Biostratigraphic analysis indicates the presence of a substantial disconformity near this horizon, presumably a result of erosion of the nannofossil ooze during a time of increased dissolution.

It is not clear why carbonate ooze provides a good environment for making large pyrite aggregates. Perhaps differences in the chemistry of microenvironments are more pronounced here than in typical hemipelagic sediments, and sites of iron sulfide precipitation are less abundant. A burrow within carbonate ooze, with relatively high sulfate reduction potential from organic matter within, may draw iron from a larger space than a burrow within hemipelagic sediments where reducing sites are more common throughout the sediment. Large pyritic aggregates are well known from both mudstones and limestones in the Jurassic sediments of southern Germany. Such aggregates are commonly associated with microfossils (the organic matter associated with these microfossils was responsible for sulfate reduction during early diagenesis).

Glauconite

Greenish small grains, apparently of authigenic origin, were observed at several sites and were reported as “glauconite” (Fig. 14). The highest values were observed at Sites 1076 and 1077 on the Congo Fan. This mineral may also be present at Site 1075, but perhaps less conspicuously. Glauconite is reported from shelf environments in regions of high productivity (to account for reduction of iron), of availability of (iron-rich) terrigenous sediments, and of low sedimentation rates. Glauconite-cemented fecal pellets are common in shelf and margin surface sediments off the Congo and Angola (Wefer and Shipboard Scientific Party, 1988). The glauconite observed at the Congo Fan sites may represent redeposition, rather than in situ growth, which may be true for the other sites as well. If so, one would expect increased abundance of glauconite during times of low sea level. At this point, no data are available to test this hypothesis.

Methane Hydrate (Clathrates)

The seismic profiles off Angola show numerous indications of vertical tectonics caused by salt diapirism and associated vertical migration and trapping of fluids and gas. Because of the fine overall grain size of the hemipelagic sediments and their low permeability, fluid/gas migration is probably restricted to areas of tectonic fracturing. In these areas, zones of high reflection and scattering amplitudes (Fig. 15) seem to indicate the presence of trapped gas at depths as shallow as 250 m. A typical continuous bottom-simulating reflector (BSR) with reversed polarity has been observed only within a restricted interval between 200 and 300 mbsf. The upper boundary generally follows the topography. BSRs off Peru and elsewhere in methane-rich regions are commonly interpreted as denoting the lower boundary of clathrate stability (Shipley et al., 1979; Kvenvolden and Kastner, 1990); that is, methane-rich water ice (with a structure different from that of regular ice). Because the region off Angola is known to be rich in hydrocarbons (it is being actively explored by oil companies), we assumed that the observations regarding an apparent BSR indicated varying abundances of clathrates within their stability field. With a gradient near 45°C/km, we should expect instability below 600 mbsf at Site 1077, for example. As previously mentioned, the depth in the section with the strong reflectors is generally shallower than 600 mbsf. However, nothing is known about lateral variability in heat flow caused by fluid/gas migration in the area.

Because of the strong reflectors and their possible association with hydrocarbons, the safety panel quite generally restricted drilling to the uppermost 200 m of the sediment column. The panel took particular care to have us avoid sites where the reflectors are especially strong, because gas pockets might be found trapped below clathrate-cemented (and therefore relatively impermeable) deposits. We were surprised, however, not to find any indication of the presence of clathrates at any of the sites drilled during Leg 175.

During the entire expedition, we looked for unusually strong gas development from the release of gas from clathrates. Such release can

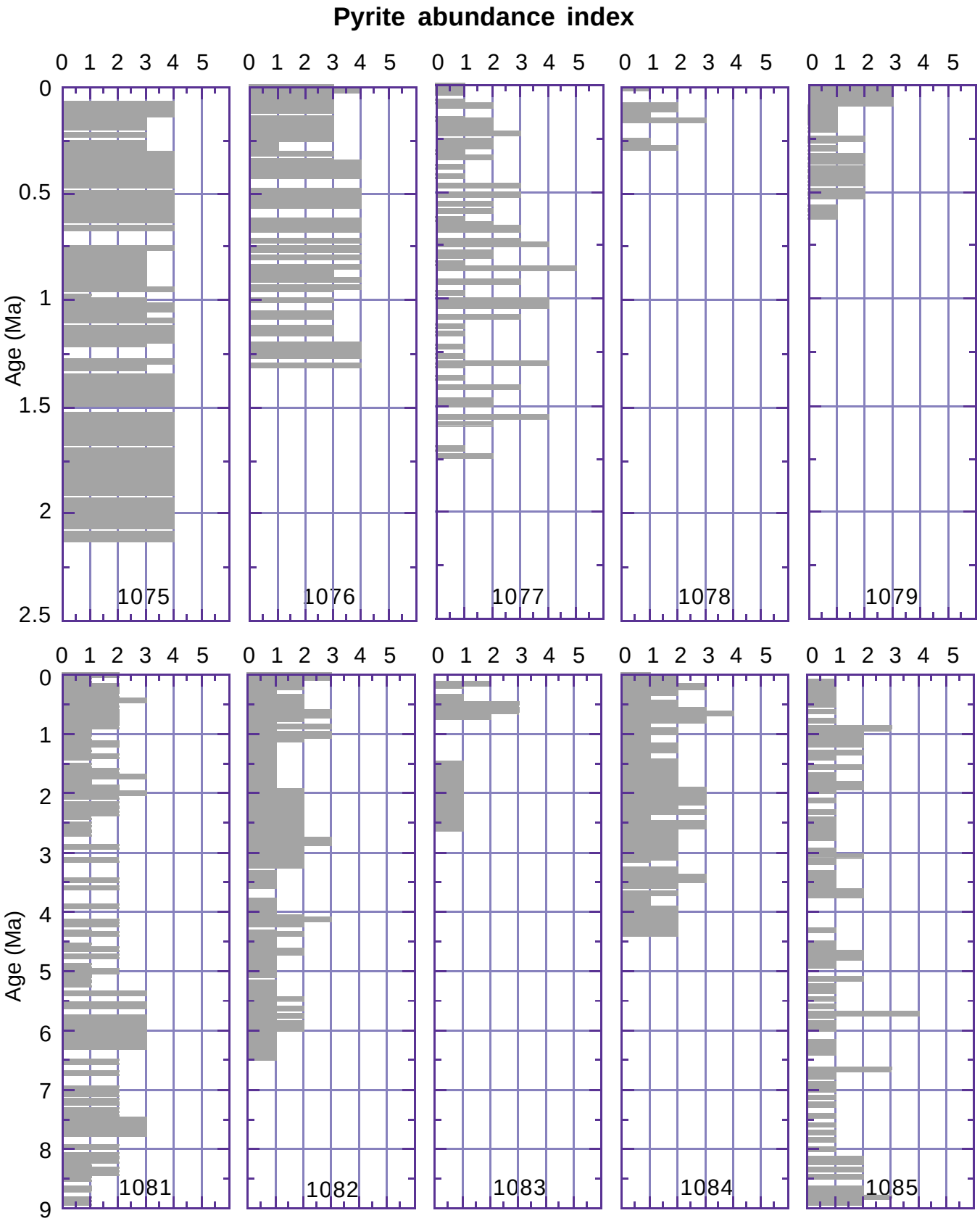

Figure 13. Abundance pattern of pyrite reported at Leg 175 Sites 1075–1085, based on smear-slide analyses (see individual site chapters, this volume).

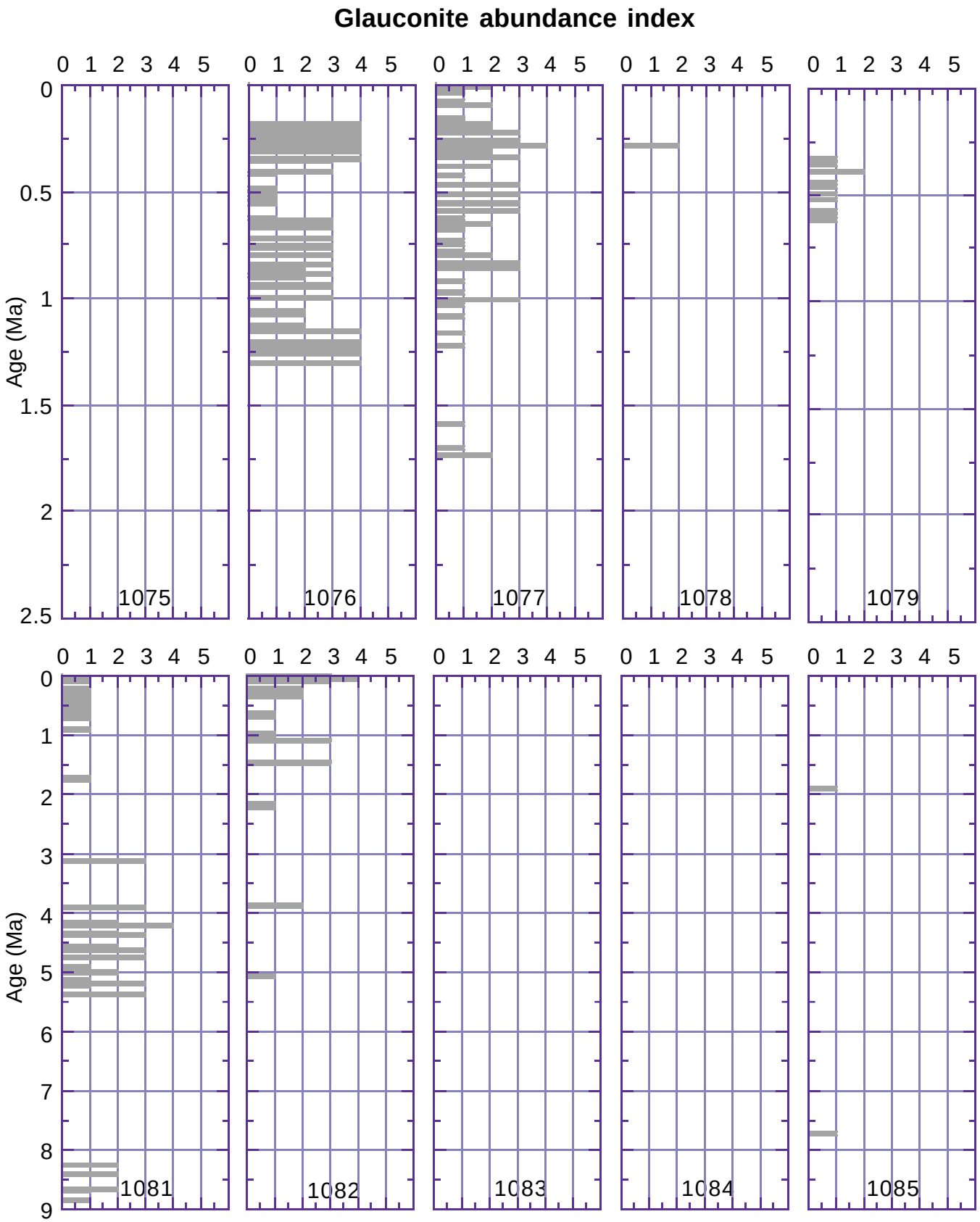

Figure 14. Abundance pattern of glauconite grains at Leg 175 Sites 1075–1085, based on smear-slide analyses (see individual site chapters, this volume).

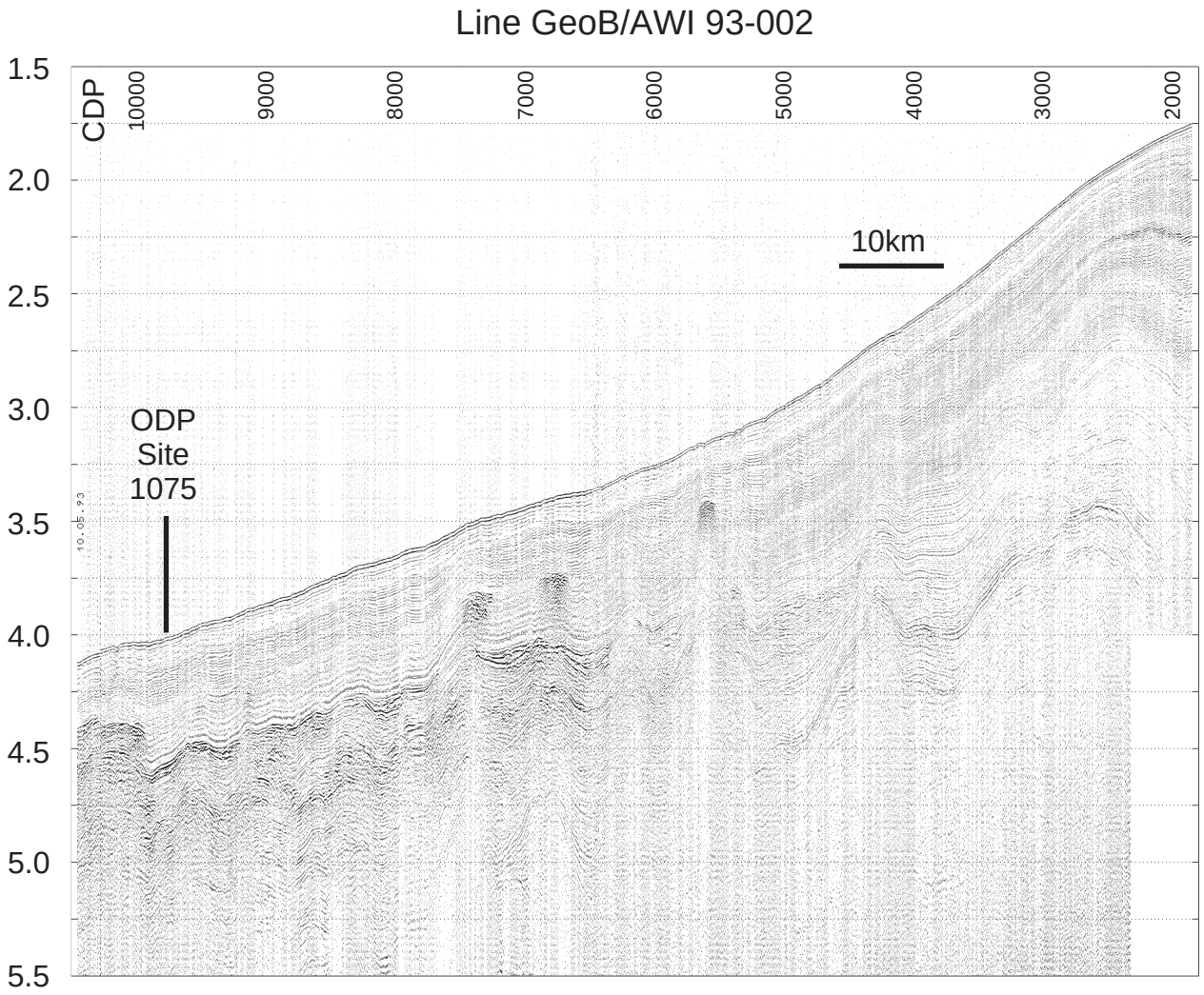

Figure 15. Seismic profile across Site 1075 showing high-amplitude "cloud" structures, presumably indicating the upper limit of a clathrate-controlled trapping zone.

be rapid and pose serious problems during handling of cores on deck (Suess, von Huene, et al., 1988). Although gas release was vigorous in many places (Meyers et al., Chap. 21, this volume), it did not seem to exceed what might be expected from normal degassing of depressurized, warming, gas-rich sediments. When clathrates melt, freshwater is added to interstitial waters (Hesse and Harrison, 1981). We found no evidence for decreases in salinity or chlorinity corresponding to an addition of freshwater from melting of clathrates in locations where clathrates might be expected (Murray et al., Chap. 20, this volume).

Our negative findings do not preclude the presence of clathrates on the continental slope off Angola, or elsewhere off southwest Africa. We have to take into account that we did not drill too deeply because of safety concerns. There could be clathrates deeper in the sediment. Certainly, methane is present in great abundance in the sediments recovered during Leg 175, and the conditions for formation of clathrates would seem to be favorable (unless dominance of CO_2 in the gases within the sediment prevents or slows the process). As discussed earlier, we expressly avoided areas near "cloud structures" and higher reflection amplitudes where clathrate might be expected to be most abundant.

CONCLUSIONS

The highlights of the sedimentological shipboard results may be summarized as follows:

1. Four different major sedimentary facies were encountered. At the northern end of the north–south transect, sediments have a large terrigenous component. On and near the Walvis Ridge, sediments have a strong pelagic aspect. South of the Walvis Ridge, sediments are unusually rich in opal and organic matter, and at the southern end of the transect, in the Southern Cape Basin, sediments are dominated by pelagic components.
2. Sedimentation rates are unusually high, ranging between 30 and 600 m/m.y. They are usually near 100 m/m.y. On the whole, the hemipelagic sites north of the Walvis Ridge have somewhat higher rates than those south of the ridge. Within the Quaternary record, hemipelagic sediments show a tendency toward increased sedimentation rates with time.
3. Organic carbon values are between 1 and 5 wt% north of the Walvis Ridge. South of the ridge, values are typically <5 wt% but can reach well over 10 wt% at sites near the coastal up-

welling areas. Black layers extremely rich in organic carbon (as much as 20 wt%) are common at the Lüderitz site (1084). Noteworthy is the overall decrease in downhole percentages. Continued diagenetic destruction of organic matter and an increase in upwelling and productivity within the last 10 m.y. are thought to be responsible for this decrease.

4. There is pervasive evidence for high productivity leading to intense chemical activity within the sediments, to the production of gas (methane and CO_2), and to the formation of new minerals (dolomite, phosphorite, glauconite, and authigenic iron sulfides), especially at sites close to the Walvis Ridge and basin and Lüderitz Bay.
5. Layers of hard rock (made of dolomite and calcite, or dolomite-cemented and calcite-cemented clay) form within soft organic-rich sediments <1 m.y. old. Logging proved extremely useful in determining the positions and thicknesses of these layers. Because of their high resistivity, they are readily identified by the FMS tool.
6. Because the region off the Congo and Angola is known to be rich in hydrocarbons, we assumed that clathrates (methane-rich water ice) are common in the sediments. A typical BSR has been observed within restricted intervals. BSRs are commonly interpreted as denoting the lower boundary of clathrate stability. We were surprised, however, not to find any indication of the presence of clathrates at any of the sites drilled during Leg 175.

REFERENCES

Baker, P.A., and Burns, S.J., 1985. The occurrence and formation of dolomite in organic-rich continental margin sediments. *AAPG Bull.*, 69:1917–1930.

Baker, P.A., and Kastner, M., 1981. Constraints on the formation of sedimentary dolomite. *Science*, 213:215–216.

Berger, W.H., 1989. Global maps of ocean productivity. *In* Berger, W.H., Smetacek, V.S., and Wefer, G. (Eds.), *Productivity of the Oceans: Present and Past:* New York (Wiley), 429–455.

Berger, W.H., and Wefer, G., 1996a. Central themes of South Atlantic circulation. *In* Wefer, G., Berger, W.H., Siedler, G., Webb, D.J. (Eds.) *The South Atlantic: Present and Past Circulation:* Berlin (Springer-Verlag), 1–11.

————, 1996b. Expeditions into the past: paleoceanographic studies in the South Atlantic. *In* Wefer, G., Berger, W.H., Siedler, G., Webb, D.J. (Eds.), *The South Atlantic: Present and Past Circulation:* Berlin (Springer-Verlag), 363–410.

Bolli, H.M., Ryan, W.B.F., et al., 1978. *Init. Repts. DSDP*, 40: Washington (U.S. Govt. Printing Office).

Burns, S.J., Baker, P.A., and Showers, W.J., 1988. The factors controlling the formation of dolomite in organic-rich sediments: Miocene Drakes Bay formation, California. *In Sedimentology and Geochemistry of Dolostones.* Spec. Publ.—Soc. Econ. Paleontol. Mineral., 43:41–52.

Calvert, S.E., and Price, N.B., 1983. Geochemistry of Namibian Shelf sediments. *In* Thiede, J., and Suess, E. (Eds.), *Coastal Upwelling: its Sedimentary Record* (Pt. A): *Responses of the Sedimentary Regime to Present Coastal Upwelling:* New York (Plenum), 337–376.

Compton, J.S., 1988. Degree of supersaturation and precipitation of organogenic dolomite. *Geology*, 16:318–321.

Compton, J.S., and Siever, R., 1986. Diffusion and mass balance of Mg during early dolomite formation, Monterey Formation. *Geochim. Cosmochim. Acta*, 50:125–135.

Curray, J.R., Moore, D.G., et al., 1982. *Init. Repts. DSDP*, 64 (Pts. 1 and 2): Washington (U.S. Govt. Printing Office).

Diester-Haass, L., Meyers, P.A., and Rothe, P., 1990. Miocene history of the Benguela Current and Antarctic ice volumes: evidence from rhythmic sedimentation and current growth across the Walvis Ridge (Deep Sea Drilling Project Sites 362 and 532). *Paleoceanography*, 5:685–707.

Garrison, R.E., Kastner, M., and Zenger, D.H., 1984. *Dolomites of the Monterey Formation and Other Organic-Rich Units.* Soc. Econ. Paleontol. Mineral., Pacific Sect., 41.

Hay, W.W., Sibuet, J.-C., et al., 1984. *Init. Repts. DSDP*, 75: Washington (U.S. Govt. Printing Office).

Henderson, N.C., Crawford, A., Punhand, J.B., and Osborne, R.H., 1984. Relationship of diagenetic dolomite to depositional facies in diatomaceous sediments, upper Sisquoc Formation, Casmalia Hill, Santa Barbara County, Calif. *In* Garrison, R.E., Kastner, M., and Zenger, D.H. (Eds.), *Dolomites in the Monterey Formation and Other Organic-rich Units.* Spec. Publ.—Soc. Econ. Paleontol. Mineral., 41:119–140.

Hesse, R., and Harrison, W.E., 1981. Gas hydrates (clathrates) causing pore-water freshening and oxygen isotope fractionation in deep-water sedimentary sections of terrigenous continental margins. *Earth Planet. Sci. Lett.*, 55:453–462.

Jansen, J.H.F., van Weering, T.G.E., Gieles, R., and van Iperen, J., 1984. Middle and late Quaternary oceanography and climatology of the Zaire-Congo fan and the adjacent eastern Angola Basin. *Neth. J. Sea Res.*, 17:201–241.

Kastner, M., Elderfield, H., Martin, J.B., Suess, E., Kvenvolden, K.A., and Garrison, R.E., 1990. Diagenesis and interstitial-water chemistry at the Peruvian continental margin—major constituents and strontium isotopes. *In* Suess, E., von Huene, R., et al., *Proc. ODP, Sci. Results*, 112: College Station, TX (Ocean Drilling Program), 413–440.

Kulm, L.D., Suess, E., and Thornburg, T.M., 1984. Dolomites in the organic-rich muds of the Peru forearc basins: analogue to the Monterey Formation. *In* Garrison, R.E., Kastner, M., and Zenger, D.H. (Eds.), *Dolomites in the Monterey Formation and Other Organic-rich Units.* Spec. Publ.—Soc. Econ. Paleontol. Mineral., 41:29–48.

Kvenvolden, K.A., and Kastner, M., 1990. Gas hydrates of the Peruvian outer continental margin. *In* Suess, E., von Huene, R., et al., *Proc. ODP, Sci. Results*, 112: College Station, TX (Ocean Drilling Program), 517–526.

Lyle, M., Koizumi, I., Richter, C., et al., 1997. *Proc. ODP, Init. Repts.*, 167: College Station, TX (Ocean Drilling Program).

Peterson, R.G., and Stramma, L., 1991. Upper-level circulation in the South Atlantic Ocean. *Progr. Oceanogr.*, 26:1–73.

Shimmield, G.B., and Price, N.B., 1984. Recent dolomite formation in hemipelagic sediments off Baja California, Mexico. *In* Garrison, R.E., Kastner, M., and Zenger, D.H. (Eds.), *Dolomites in the Monterey Formation and Other Organic-rich Units.* Spec. Publ.—Soc. Econ. Paleontol. Mineral., 41:5–18.

Shipley, T.H., Houston, M.H., Buffler, R.T., Shaub, F.J., McMillen, K.J., Ladd, J.W., and Worzel, J.L., 1979. Seismic evidence for widespread possible gas hydrate horizons on continental slopes and rises. *AAPG Bull.*, 63:2204–2213.

Siesser, W.G., 1978. Petrography and geochemistry of pyrite and marcasite in Deep Sea Drilling Project Leg 40 sediments. *In* Bolli, H.M., Ryan, W.B.F., et al., *Init. Repts. DSDP*, Suppl. to Vols. 38, 39, 40, and 41: Washington (U.S. Govt. Printing Office), 767–775.

————, 1980. Late Miocene origin of the Benguela upwelling system off northern Namibia. *Science*, 208:283–285.

Suess, E., von Huene, R., et al., 1988. *Proc. ODP, Init. Repts.*, 112: College Station, TX (Ocean Drilling Program).

————, 1990. *Proc. ODP, Sci. Results*, 112: College Station, TX (Ocean Drilling Program).

Wefer, G., and Shipboard Scientific Party, 1988. Bericht über die METEOR-Fahrt M6/6, Libreville - Las Palmas, 18.2–23.3. 1988. *Ber. Fachbereich Geowiss. Univ. Bremen, Germany*, 3.

Ms 175IR-116